JCI insight

A20 and the non-canonical NF-κB pathway are key regulators of neutrophil recruitment during fetal ontogeny

Ina Rohwedder, … , Matthias Heinig, Markus Sperandio

JCI Insight. 2023. https://doi.org/10.1172/jci.insight.155968.

Research In-Press Preview **Inflammation**

Graphical abstract

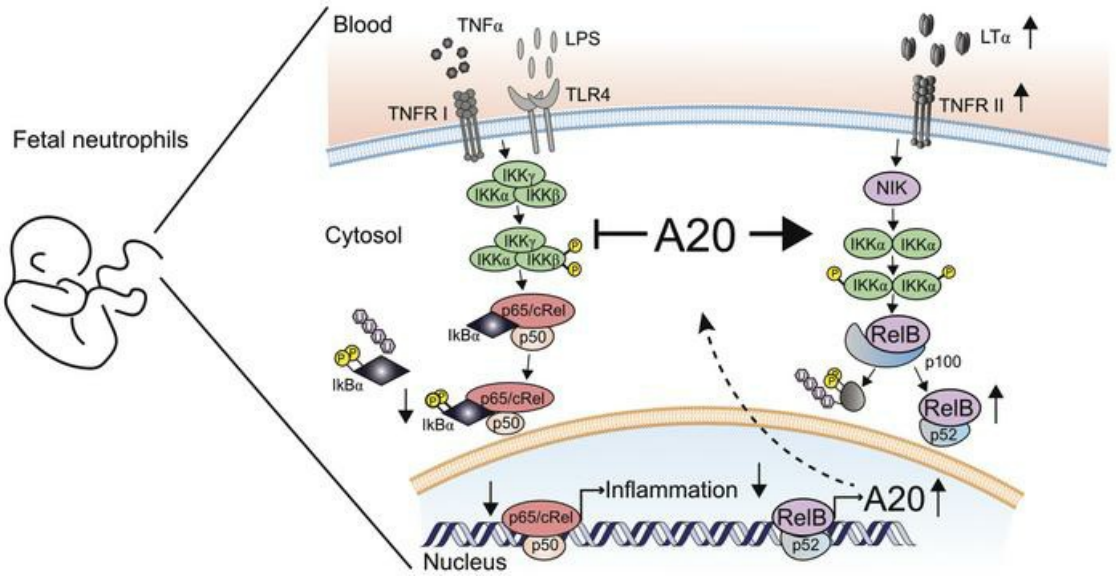

Find the latest version:

https://jci.me/155968/pdf

A20 and the non-canonical NF-κB pathway are key regulators of neutrophil recruitment during fetal ontogeny

Ina Rohwedder[1*], Lou Martha Wackerbarth[1*], Kristina Heinig[1], Annamaria Ballweg[1], Johannes Altstätter[1], Myriam Ripphahn[1], Claudia Nussbaum[2], Melanie Salvermoser[1], Susanne Bierschenk[1], Tobias Straub[3], Matthias Gunzer[4,5], Marc Schmidt-Supprian[6], Thomas Kolben[7], Christian Schulz[8] Averil Ma[9], Barbara Walzog[1], Matthias Heinig[10,11] and Markus Sperandio[1#]

[1]Institute of Cardiovascular Physiology and Pathophysiology, Walter-Brendel-Center of Experimental Medicine, LMU Munich, Martinsried, Germany, [2]Division of Neonatology, Dept. of Pediatrics, Dr. von Hauner Children's Hospital LMU Munich, Munich, Germany, [3]Core Facility Bioinformatics, BMC, LMU Munich, Martinsried, Germany, [4]Institute for Experimental Immunology and Imaging, University of Duisburg-Essen, Essen, Germany, [5]Leibniz-Institut für Analytische Wissenschaften ISAS -e.V, Dortmund, Germany, [6]Department of Hematology and Medical Oncology, TU Munich, Munich, Germany, [7]Department of Gynecology and Obstetrics, University Hospital, LMU Munich, Munich, Germany, [8]Medical Clinic I., University Hospital, LMU Munich, Munich, Germany, [9]Department of Medicine, University of California, San Francisco, San Francisco, CA, [10]Institute of Computational Biology, Helmholtz Zentrum, Munich, Germany, [11]Department of Informatics, Technical University Munich, Munich, Germany.

[*] *contributed equally*

[#] *corresponding author*

ORCIDs:

I.R: 0000-0002-5833-4279, M.S.: 0000-0002-7689-3613; M.G.: 0000-0002-5534-6055, C.S.: 0000-0002-8149-0747

Correspondence:

Markus Sperandio, M.D.

Institute of Cardiovascular Physiology and Pathophysiology

Biomedizinisches Centrum München

Ludwig-Maximilians-Universität

Großhaderner Str. 9

82152 Planegg-Martinsried

GERMANY

voice: +49 (0)89 2180 71513

Fax: +49 (0)89 2180 71511

Email: markus.sperandio@lmu.de

Key words: NF-κB pathway, A20, neutrophils, fetal immune system

Category of the manuscript: Original article

Summary: The non-canonical NF-κB pathway and the ubiquitin modifying enzyme A20 are key regulators keeping fetal neutrophils in a non-responsive state by downregulating the inflammatory response during fetal ontogeny.

Abstract

Newborns are at high risk of developing neonatal sepsis, particularly if born prematurely. This has been linked to divergent requirements the immune system has to fulfill during intrauterine compared to extrauterine life. By transcriptomic analysis of fetal and adult neutrophils we set out to shed new light on the molecular mechanisms of neutrophil maturation and functional adaption during fetal ontogeny. We identified an accumulation of differentially regulated genes within the non-canonical NF-κB signaling pathway accompanied by constitutive nuclear localization of RelB and increased surface expression of TNFRII in fetal neutrophils as well as elevated levels of LT-α in fetal serum. Furthermore, we found strong upregulation of the negative inflammatory regulator A20 (*Tnfaip3*) in fetal neutrophils, which was accompanied by pronounced downregulation of the canonical NF-κB pathway. Functionally, overexpressing A20 in Hoxb8 cells led to reduced adhesion of these neutrophil-like cells under flow. Conversely, mice with a neutrophil specific A20 deletion displayed increased inflammation in vivo. Taken together, we have uncovered constitutive activation of the non-canonical NF-κB pathway with concomitant upregulation of A20 in fetal neutrophils. This offers perfect adaption of neutrophil function during intrauterine fetal life, but also restricts appropriate immune responses particularly in prematurely born infants.

Introduction

Prematurely born infants are highly susceptible to bacterial, fungal and viral infections and have an increased morbidity and mortality from neonatal sepsis compared to term babies (1,2). This clinical observation reflects the contrasting requirements the immune system has to fulfill to guarantee normal growth and development during intrauterine life on one hand and on the other hand, to cope with the challenges and threats, infants are exposed to in the outside world after birth (3),(4). For the innate immune system, one of the key players in host defense are neutrophils, that, upon an inflammatory stimulus are attracted to the site of inflammation by a well-orchestrated recruitment process that finally leads to their extravasation from the blood stream into inflamed tissue (5,6). This recruitment process is severely restricted during early stages of fetal development when compared to adults (7,8). As a functional consequence, murine and human fetal neutrophils display a limited capacity to roll and adhere in vitro and in vivo. Interestingly, exposure to the extrauterine environment as in prematurely born infants does not stimulate neutrophil function, but instead, neutrophil maturation seems to be regulated by an intrinsic molecular program (7). Recently, using various systems biology approaches, several studies have investigated immune system development during the neonatal period (9–11). Besides an increase in type I IFN-related functions, an ontogenetic control of neutrophil signaling was suggested targeting Toll-like receptor- and IL1-dependent signaling, both of which affecting the NF-κB signaling pathways (9).

The NF-κB family of transcription factors is ubiquitously expressed and regulates numerous targets particularly in immune cells (12). Two major signaling pathways exist: the canonical and the non-canonical form. The canonical signaling pathway is activated downstream of inflammatory surface receptors on immune cells including Toll-like receptors (TLRs) or the Tumor necrosis factor alpha (TNF-α) receptor and leads to nuclear translocation of the NF-κB subunit p65. It initiates the rapid but transient activation of gene transcription of proinflammatory cytokines and therefore induces and prolongates the inflammatory response. In contrast, RelB, known as the primary effector of the non-canonical NF-κB signaling pathway, initiated by a diverse range of ligands and receptors, like LTβR/LT-α1β2 or TNFR II/LT-α elicits a slow and persistent activation of gene transcription (13). While the non-canonical NF-κB signaling pathway is well known for its importance in lymph node development during fetal ontogeny (14), it also functions as a fine-tuning mechanism for inflammatory responses. This was shown by chromatin immunoprecipitation (ChIP) sequencing that revealed numerous RelB downstream targets, among them important immune modulators such as IRAK-3 and the ubiquitin modifying enzyme A20 (gene name: tumor necrosis factor-alpha-induced protein 3, *TNFAIP3*) (15). A20 is a key negative feedback inhibitor of the canonical NF-κB signaling pathway exerting its immunomodulatory function through its ubiquitin modifying properties (16–18). Accordingly, A20 deficiency in mice resulted in multiorgan inflammation and premature death (19). Further studies using conditional knockout mice focused on the role of A20 in innate immune cells. Mice with an A20 deficiency (*Tnfaip3*$^{-/-}$ mice) in the myeloid compartment developed spontaneous polyarthritis with sustained proinflammatory cytokine production (20).

Using a whole transcriptome analysis approach, we aimed to investigate the molecular mechanisms regulating neutrophil maturation during fetal development and found a robust upregulation of RelB target genes in fetal neutrophils including A20. Furthermore, we could observe nuclear accumulation of RelB in fetal neutrophils suggesting constitutively active non-canonical NF-κB signaling and A20 as a key modifier of neutrophil function during fetal ontogeny.

Results

Differential gene expression signatures in human fetal and adult neutrophils.

Fetal neutrophils from early embryonic stages display a reduced capacity to react to inflammatory stimuli, thus leaving the organism highly vulnerable to invading pathogens or sterile inflammation. This study aimed to investigate the underlying molecular mechanisms regulating fetal neutrophil function during ontogeny. We therefore performed whole transcriptome analysis of human fetal cord blood-derived neutrophils from premature (<37 weeks of gestation) and mature (>37 weeks of gestation) infants and compared their gene expression profiles to neutrophils from healthy adult donors (Figure 1A). Flow cytometric analysis and cytospin was used to ensure that comparable cell populations of human adult and mature fetal neutrophils were included in the analysis (Supplemental Figure 1A and B). We identified 124 differentially regulated genes (FDR < 5%, Figure 1A), 56 were upregulated and 68 were downregulated in fetal vs. adult neutrophils. To understand the biological significance underlying these differentially regulated genes and provide a rough overview, we applied WEB-based Gene SeT AnaLysis Toolkit (WebGestalt), that allowed us to group our candidate genes according to their function and association with biological processes (Figure 1B and Supplemental Table 1). Strikingly, the analysis revealed that most prominent changes in identified gene sets occurred for those sets of genes with negative regulatory functions in cellular defense and activation as well as protein trafficking.

The non-canonical NF-κB subunit RelB determines a specific gene expression signature in fetal human neutrophils.

Next, we analyzed the differentially regulated genes found in our transcriptomic screen in more detail. We could associate several of the differentially regulated genes (including *TNFAIP3*, *IRAK3*, *RELB*) to the NF-κB signaling pathway. This prompted us to systematically assess whether binding sites of NF-κB subunits in GM12878 human lymphoblastoid B cells (15) were overrepresented at promoters of genes that were upregulated or downregulated in fetal neutrophils in comparison to adult neutrophils. RelB was the subunit with strongest overrepresentation in promoters of upregulated genes ($P = 5.19 \times 10^{-7}$FET, OR=4.0, Supplemental Table 2). Using this approach, we were able to identify a total of 40 RelB target genes, that were upregulated in fetal neutrophils compared to their adult counterparts and additional 24 RelB target genes displaying the opposite signature with lower expression in fetal neutrophils (Figure 2A, Supplemental Table 3). This means that 71% of all fetal upregulated genes and 35% of all fetal downregulated genes are associated with the RelB pathway.

Upon activation of the non-canonical NF-κB signaling pathway the transcription factor RelB is translocated from the cytoplasm into the nucleus to induce gene transcription. In order to test for baseline activation of the non-canonical pathway, we analyzed RelB localization in fetal and adult human neutrophils using imaging flow cytometry (AMNIS). This allows us to assess the subcellular localization of RelB on a large cell population. We were able to detect co-localization of RelB to the DAPI-stained nucleus of premature and mature fetal neutrophils, while this was significantly reduced in adult neutrophils (Figure 2B and C). In addition, we could see the same increased co-localization of RelB to the DAPI-stained nucleus in murine fetal neutrophils compared to adult cells (Supplemental Figure 1C). Furthermore, the canonical NF-κB subunit p65 was not differentially co-localizing to the nucleus in fetal or adult neutrophils suggesting an

exclusive baseline activation of the non-canonical NF-κB signaling pathway in human fetal neutrophils (Supplemental Figure 1D). We then quantified total RelB protein in our samples and could observe no significant alterations in overall RelB expression in fetal vs. adult neutrophils, although a tendency towards increased RelB amount was detected in samples from premature infants (Supplemental Figure 1E). In resting cells, RelB activation and translocation is inhibited by its binding to p100. Upon activation of the non-canonical NF-κB signaling pathway, p100 is in part proteasomally degraded into p52, and subsequently, as a dimer with RelB, translocated into the nucleus. In accordance to our previous results, we detected significantly higher baseline levels of cleaved p52 in fetal neutrophils compared to adult neutrophils by western blot analysis, with the highest values in early premature samples under 37 weeks of gestational age (Figure 2D). As these results indicate that in fetal neutrophils NF-κB signaling is shifted towards the non-canonical pathway, we were interested in upstream factors inducing this pathway. While TLR4 and the TNF-receptor are well-known inducers of the canonical NF-κB signaling pathway, there are also a variety of receptors that differentially induce the non-canonical pathway including CD40, Ox40, RANK, LTβR and TNFRII being expressed on neutrophils. Using flow cytometry analysis, we could detect expression of TNFRII (Figure 2E) and LTβR (Supplemental Figure 2A) on fetal and adult human as well as murine neutrophils. Interestingly, TNFRII displayed significantly higher surface expression levels in human samples obtained at a gestational age under 37 weeks compared to adult (Figure 2E left graph), with a similar tendency, although not significant, in murine samples (Figure 2E right graph). One of the ligands for TNFRII is lymphotoxin α (LT-α), well known for its role in the development of secondary lymphatic tissue (21). We analyzed serum levels of LT-α in cord blood serum of human premature and mature infants as well as in adult serum using quantitative ELISA. We detected significantly higher LT-α serum levels in cord blood of premature and mature infants than in samples from adults (Figure 2F) suggesting that the LT-α/TNFRII axis might play a critical role in the observed elevated baseline activation of the immunomodulatory non-canonical NF-κB signaling pathway in fetal neutrophils.

Downregulation of the canonical NF-κB signaling pathway in fetal neutrophils.

Because of the described immune-modulatory function of the non-canonical NF-κB signaling pathway and its antagonizing effects on canonical NF-κB signaling, we wanted to test, whether fetal neutrophils also display reduced inflammation-driven activation of the canonical NF-κB pathway. To address this, we stimulated fetal and adult human neutrophils for 20 minutes with 10ng/ml TNF-α, which induces canonical signaling via the TNF-receptor. Upon activation of the TNF-receptor, a series of kinases is activated resulting in the phosphorylation of IκBα, IκBβ and IκBγ, leading to their proteasomal degradation and release of p65 and p50 heterodimers. While TNF-α stimulation resulted in a robust phosphorylation of IκBα in adult neutrophils (Figure 3A), we were unable to observe a similar increase in phosphorylation in fetal samples, indicating that fetal neutrophils are less capable to activate the canonical signaling cascade upon stimulation. This observation is not due to a differential expression of the TNF1 receptor (TNFR I) on the neutrophil surface (Supplemental Figure 2B), suggesting an intracellular regulatory mechanism. Additionally, stimulation with TNF-α was unable to induce upregulation of Mac-1 ($\alpha_M\beta_2$, CD11b/CD18) surface levels in human fetal neutrophils to the same extend as in adult neutrophils (Figure 3B). Surface expressed Mac-1 has been demonstrated to be critical for neutrophil recruitment into inflamed tissue(22). Hypothesizing, that factors in fetal serum like LT-α keep fetal neutrophils in a less activatable state, we stimulated adult neutrophils with fetal or adult serum and analyzed the levels of phosphorylated IκBα and

p52 as well as neutrophil effector functions (Figure 3C). Incubating neutrophils with fetal serum showed diminished phosphorylation of IκBα compared to stimulation with adult serum. When being stimulated with fetal serum, p52 protein levels increased compared to controls (Figure 3D and E) indicating that fetal serum induces a shift in adult neutrophils towards the non-canonical signaling pathway, keeping neutrophils in a rather unresponsive state towards inflammatory stimuli. We performed the same experiment as described before on fetal human neutrophils and could see that adult human serum is able to switch fetal neutrophils to a proinflammatory state with upregulated pIκB levels (Supplemental Figure 2C). This again reinforces our hypothesis that factors like LT-α in the fetal serum are able to dampen the inflammatory NF-κB induced response. Interestingly, incubation of human adult neutrophils with recombinant human LT-α for 2h was also able to prevent canonical NF-κB signaling via TNF-α (Figure 3F), as shown by strongly reduced phosphorylation levels of IκBα.

Next, we investigated if incubation of human adult neutrophils with fetal serum is also affecting other neutrophil functions and tested neutrophil adhesion using flow chambers coated with rhICAM-1/rhE-selectin and rhCXCL8 as a substrate for adhesion. These experiments showed that adult neutrophils incubated with fetal serum displayed reduced adhesion in the flow chamber compared to cells incubated with adult serum indicating that fetal serum has the capacity to reduce neutrophil adhesion under flow (Figure 3G).

Using the Zymosan uptake assay we then analyzed phagocytosis of human adult neutrophils after incubation with fetal serum. Again, fetal serum incubation was able to reduce phagocytosis of Zymosan by adult neutrophils (Figure 3H) providing evidence that various neutrophil functions are altered in the presence of fetal serum. Blocking TNFRII on human adult neutrophils using an anti-human TNRFII antibody was able to prevent the inhibitory activity of fetal serum, since phagocytic activity of adult neutrophils stimulated with fetal serum was significantly increased after blocking of TNFRII beforehand. Adult neutrophils in the presence of adult serum after blocking the TNFRII receptor did not show increased phagocytic activity verifying an important role of the LT-α/TNFRII axis in modulating fetal neutrophil function (Supplemental Figure 2D). Next, we applied an in vivo model of fetal inflammation and performed intravital imaging experiments on neutrophil adhesion in inflamed mouse yolk sac vessels 2h after intrauterine LPS (100µg) stimulation. These experiments were conducted with *Lyz2*^{GFP} mice (23), where neutrophils harbor a bright GFP signal. LPS via binding to TLR4 is one of the main activators of the canonical NF-κB signaling pathway, inducing a proinflammatory MyD88-dependent transcriptional program that consequently results in the activation of neutrophils and endothelial cells inducing neutrophil adhesion to the inflamed endothelium. While in E14.5 yolk sac vessels only very few leukocytes interacted with the vessel wall after LPS stimulation (Supplemental Movie 1 and Figure 3I), we were able to detect significantly higher numbers of adherent cells at yolk sac vessels of E17.5 fetuses compared to control stimulation using normal saline (Supplemental Movie 2). We also applied TNF-α in E14.5 and E17.5 fetuses and obtained similar numbers of adherent cells as in LPS stimulated fetuses (Figure 3J). To exclude differences in the expression of TLR4 on the neutrophil surface of E14.5 vs. E17.5 fetuses, we performed flow cytometry analysis, which revealed similar expression of TLR4 on neutrophils from E14.5 and E17.5 fetuses compared to neutrophils from adult mice (Supplemental Figure 2E). Adhesion to inflamed vessels critically depends on the interaction between endothelial ICAM-1 and LFA1 (integrin $\alpha_L\beta_2$), expressed on neutrophils. Thus, we analyzed the capacity of E14.5, E17.5 and adult neutrophils to bind soluble rmICAM-1 (rmICAM-1 hFC chimera) in vitro. As expected, stimulation of neutrophils with the chemokine CXCL-1 or

using PMA induced an increase in ICAM-1 binding due to LFA1 activation in adult neutrophils, but this effect was severely reduced in neutrophils from E14.5 or E17.5 fetuses (Supplemental Figure 2F).

A20 upregulation in fetal neutrophils results in diminished adhesion.

So far, our results revealed that fetal neutrophils exhibit a pronounced baseline activation of the non-canonical NF-κB signaling pathway. Several of the RelB target genes identified in the transcriptomic analysis have immunomodulatory functions and are able to suppress the inflammatory canonical NF-κB signaling pathway. One of those upregulated RelB target genes in fetal neutrophils and detected in the transcriptomic analysis was the ubiquitin modifying enzyme A20, which has been reported as key negative regulator of innate immune responses. A20 might therefore be an interesting candidate in down-modulating innate immune responses during fetal life. To test this, we first validated A20 upregulation in fetal human neutrophils by RT-PCR (Figure 4A) and additionally on the protein level in comparison to adult neutrophils (Figure 4B). We found a significant upregulation of A20 on the transcriptional as on the protein level in fetal neutrophils. Next, we investigated A20 levels in the mouse and confirmed our findings in human neutrophils with increased levels of A20 mRNA in fetal vs. adult mouse neutrophils (Figure 4C). Interestingly, A20 levels gradually started to decrease at late embryonic stages (E14.5 vs. E17.5), which is in line with our in vivo findings of increased adhesion after LPS or TNF-α stimulation at E17.5 vs E14.5. Thus, we conclude, that through downregulating A20 expression later during fetal ontogeny, neutrophil adhesiveness increases at the same time. To strengthen this hypothesis, we generated A20-overexpressing Hoxb8 cells and analyzed the adhesive behavior of these cells in a flow chamber system (Figure 4D). Vector transfected cells without the A20 coding region served as controls. Differentiated Hoxb8 cells have been used as an in vitro and in vivo model system to investigate neutrophil function in mice (24). Western blot analysis of A20-overexpressing differentiated Hoxb8 cells clearly showed a strong upregulation of A20 protein compared to control cells (Figure 4E). To test whether overexpression of A20 influences the adhesive behavior of differentiated Hoxb8 cells, we coated microflow chambers with rmE-selectin, rmICAM-1 and rmCXCL1 to mimic the inflamed endothelium and introduced differentiated A20-overexpressing or differentiated control Hoxb8 cells into the chambers at a defined shear rate (1dyne/cm^2). Analysis of the number of adherent cells / FOV revealed a significant decrease in adhesion of A20-overexpressing cells (Figure 4F) suggesting that A20 is a negative regulator of neutrophil adhesion.

Increased neutrophil recruitment in *Tnfaip3*$^{fl/fl}$ *Ly6gCre* mice in vivo.

In the next set of experiments, we investigated A20 depleted neutrophils in an in vivo setting of sterile inflammation. Previous observations on A20 depleted immune cells described hyperinflammation in different end-point mouse models, but so far, the impact of A20 deficiency on the leukocyte adhesion cascade itself is not known. As the A20 constitutive knockout is prematurely lethal (19), we bred *Tnfaip3*$^{fl/fl}$ mice to *Ly6g-tdTomatoCre* mice (*Tnfaip3*$^{fl/fl}$ *Ly6gCre*), to obtain mice with a highly specific deletion of A20 in mature neutrophils. We first verified A20 depletion in our model and observed a strong decrease in A20 mRNA in neutrophils derived from *Tnfaip3*$^{fl/fl}$ *Ly6gCre* mice, although a complete knockout was not achieved (Supplemental Figure 3A). Using intravital microscopy of TNF-α-stimulated cremaster muscle, we found no differences in the numbers of rolling neutrophils in *Tnfaip3*$^{fl/fl}$ *Ly6gCre* mice after normalization to the white blood cell count (WBC) compared to *Ly6gCre* mice (Figure 5A and Supplemental Movie 3). Interestingly, neutrophil rolling velocity was not altered between the groups

(Supplemental Figure 3B). Next, we analyzed neutrophil adhesion and found a significant increase in absolute numbers of adherent neutrophils/mm^2 in *Tnfaip3*$^{fl/fl}$ *Ly6gCre* mice compared to the control group (Figure 5B) suggesting that loss of A20 in neutrophils leads to a hyperreactive phenotype with increased adhesion to inflamed microvessels. Finally, we stained the exteriorized and fixed cremaster muscle tissue with Giemsa to visualize extravasated neutrophils. Again, we detected a 30% increase of extravasated neutrophils in *Tnfaip3*$^{fl/fl}$ *Ly6gCre* mice compared to *Ly6gCre* mice (Figure 5C and D). The hemodynamic parameters of both groups did not differ (Table 1). In a second set of in vivo experiments using the cremaster muscle model, experiments were performed within 45 minutes after surgical preparation of the cremaster muscle without additional stimulation. In this mild inflammation model, neutrophil-endothelial interactions are mostly limited to P-selectin dependent rolling with a few adherent neutrophils (25). Again, hemodynamic parameters were equal in *Tnfaip3*$^{fl/fl}$ *Ly6gCre* mice compared to *Ly6gCre* mice (Table 2). Interestingly, we observed decreased rolling velocities along with increased adhesion of A20 deficient neutrophils compared to *Ly6gCre* controls (Supplemental Figure 3C and D) suggesting a neutrophil-intrinsic hyperreactive phenotype in the absence of A20, which is the contrary effect of what we observed in fetal neutrophils with high A20 expression.

Discussion

In this study, we aimed to decipher the molecular mechanisms behind the ontogenetic regulation of neutrophil function during fetal development. In a whole transcriptomic survey, we identified over 120 differentially regulated genes in fetal vs. adult human neutrophils. Many of those genes upregulated in fetal samples are RelB target genes that together with elevated nuclear RelB localization and higher p52 values suggest a constitutively active non-canonical NF-κB signaling pathway in fetal neutrophils. In contrast, we observed reduced canonical NF-κB signaling in fetal neutrophils upon stimulation and diminished activation of neutrophil adhesion in an intravital microscopy model of the mouse yolk sac of E14.5 fetuses upon intrauterine LPS stimulation. Interestingly, among upregulated genes in fetal neutrophils we found the ubiquitin modifying enzyme A20 that is a well-established and potent negative regulator of the inflammatory canonical NF-κB pathway. Indeed, we generated Hoxb8 cells and showed that overexpressing A20 mimics fetal neutrophils and their inability to properly interact with immobilized adhesion molecules in a flow-chamber system. On the contrary, murine neutrophils lacking A20 showed a hyperinflammatory phenotype with increased adhesion to inflamed microvessels and extravasation into inflamed cremaster muscle tissue.

Neutrophils are among the body's first line of defense against invading pathogens. Thus, proper function of neutrophils is critical to re-establish homeostasis without harming the body. Prematurely born infants, especially those born under 33 weeks of gestation, harbor a great risk of infections or sepsis (26). This enhanced susceptibility has been linked to lacking maternal antibodies (27) but also to their immature innate immune system compared to term born infants (28). It has been shown, that under artificial shear stress, neutrophils from mature born infants demonstrate reduced adhesion compared to adult neutrophils (29), an effect which is even more pronounced in premature neutrophils (7), suggesting an ontogenetic regulation of neutrophil function. Also on the level of direct host defense, immature neutrophils lack functionality, as it was shown by reduced NET formation capability in neonates (30,31). Interestingly, the molecular mechanisms regulating this ontogenetic maturation are still incompletely understood (28). Using a systems biology approach, a recent study by the Kollmann group investigated peripheral blood samples of newborn infants during the first week of life (9). They performed transcriptomic, proteomic and metabolomic analyses and revealed a dynamic developmental trajectory affecting the interferon and complement pathway. In addition, the analysis also found changes in neutrophil-associated signaling processes affecting TLR-2 and -9 as well as IL-1-dependent signaling (9). In another recent study, Olin and colleagues investigated immune cell populations and selected plasma proteins during the first three months of life in preterm and term infants using mass cytometry (10). The authors identified a rather stereotypic postnatal development of the immune system along one shared trajectory. Interestingly, the authors found a complete segregation of 267 investigated plasma proteins and detected significant lower neutrophil numbers at birth between preterm and term infants (10). Furthermore, they uncovered upregulation of IFN-γ and CXCL8 production with increasing maturation. Of note, cord blood measurements of the immune system did not correlate well to the immune system status postnatally, which the authors traced back to multifactorial perinatal changes.

To shed new light on the regulation of neutrophils function particularly during human fetal ontogeny, we performed a whole transcriptome approach. To do this, we analyzed neutrophils derived from cord blood of premature and mature infants and compared it to blood-isolated neutrophils from adults, in search for genes that might explain the observed functional difference between fetal and adult neutrophils. Out of

124 differentially regulated genes, we found a prominent cluster of 64 genes that are associated to the NF-κB / RelB pathway (15). Furthermore, our results show higher nuclear RelB levels in fetal samples as well as higher p52 values, indicating an upregulation of the non-canonical NF-κB pathway. Unlike the canonical, inflammatory NF-κB pathway, non-canonical signaling is more diverse, ranging from secondary lymphotic tissue development, to circadian rhythm, but also acts as a modulator of immune response (13). While the role of RelB in the myeloid compartment is less known, studies on RelB single and RelB / p50 double knockout mice revealed that RelB also represses excessive neutrophil recruitment (32,33). Those findings suggest that an upregulation of RelB target genes in neonatal neutrophils could act as immune-suppressors of the canonical NF-κB pathway. Our result further lead to the assumption that elevated factors in fetal serum, like LT-α and an accompanying stronger surface expression of the TNFRII receptor could initiate this increased signaling. Monocytes from preterm infants were shown to display a diminished TLR4 expression and MyD88 signaling, along with decreased cytokine production (34,35). Similar observations were made for neutrophils derived from premature infants (36). Also in our experiments, TNF-α signaling via TNFR led to decreased IκB phosphorylation that would be required to initiate p65 nuclear translocation. This corroborates our hypothesis of a reduced canonical NF-κB signaling in fetal neutrophils as a consequence of immunosuppressive factors transcribed by the RelB pathway. We additionally show that stimulating adult neutrophils with fetal serum for 2h is significantly inhibiting IκB phosphorylation and at the same time, elevated p52 levels, as an indicator of increased non-canonical signaling. This silencing of myeloid cells observed in our study is supported by a recent report demonstrating that under baseline conditions, TLR4 induced IL1β production as well as the biological relevant secretion of cleaved IL1β is diminished in neonatal monocytes due to impaired formation of the NLRP3 inflammasome protein complex (37). Considering the fact that pathological high levels of cord blood IL1β are linked to organ damage in the fetus/newborn (38), tuning down innate immune cell function appears to be beneficial for normal fetal development in its physiological environment. We further verified this by intravital imaging of neutrophil recruitment in yolk sac vessels where we demonstrated an ontogenetic regulation of neutrophil adhesiveness following local LPS stimulation.

Among our RelB target genes that were ontogenetically upregulated in fetal neutrophils, we found the ubiquitin modifying enzyme A20, a complex regulator of NF-κB signaling. Due to its structure, A20 is able to cleave ubiquitin chains, while at the same time acting as an ubiquitin E3 Ligase and binding ubiquitin chains. Therefore, A20 interferes with and modifies ubiquitylated proteins and by this regulates NF-κB signaling in multiple ways. Originally, it was described to be activated by the canonical pathway itself (39) and is now well-accepted as a negative feedback regulator, that silences the initiated inflammatory response (40,41) and at the same time activates non-canonical NF-κB signaling (42). In A20 overexpressing HEK293 cells, TNF induced NF-κB activation is abolished (40) in the same fashion as we observed in fetal samples that harbor high A20 expression. To show the functional consequences of high A20 protein levels on immune cell function, we generated A20 overexpressing Hoxb8 cells and observed a decreased adhesion in a flow-chamber system. This further strengthens the suggested role of A20 as a key factor that switches fetal neutrophils towards the non-canonical NF-κB pathway and keeps the canonical NF-κB pathway constitutively silent. On the other hand, loss of A20 function due to truncated gene variants or SNPs are associated with auto-inflammatory disorders like Crohn's disease, psoriasis, rheumatoid arthritis and many more (16,43–46). This can also be observed in mice, either with constitutive A20 depletion (19), or with conditional deletion in the hematopoietic compartment (20,47–50). Interestingly those mice also

display increased IL1 secretion and increased basal and LPS-induced expression levels of the inflammasome adapter NLRP3 (51,52). Those previous findings of hyperinflammation in various disease models led us to investigate the neutrophil recruitment cascade itself in the absence of A20, anticipating also here an overactive inflammatory phenotype. As expected, we observed more adhesion and transmigration of A20-depleted neutrophils compared to control animals.

Taken together, we provide mechanistic insights into the ontogenetic regulation of neutrophils during fetal life and uncover a shift in NF-κB signaling towards the anti-inflammatory non-canonical NF-κB pathway that is accompanied by transcriptional upregulation of A20, a powerful negative regulator of the inflammatory response. In consequence, fetal neutrophils are restricted in their reactivity towards inflammatory signals that would finally lead to neutrophil adhesion and transmigration into inflamed tissue. While this seems to be highly beneficial for the fetus within its protected intrauterine environment, it leads to a substantial increase in morbidity and mortality in prematurely born infants facing the outside world with all its challenges and threats.

Material/Methods

Sample collection and study population

All cord blood samples used in the study were obtained from neonates delivered by Caesarean section. Immediately after delivery, blood was taken in citrate-buffer containing collection tubes or serum collecting tubes (S-Monovette, Sarstedt, Nümbrecht). Exclusion criteria included congenital malformations, known infections of the mother and familial immune diseases. Blood from adult healthy donors was taken by venipuncture.

Microarray and data processing

Human fetal and adult neutrophils were purified and RNA was isolated as described below. RNA was loaded on a Hgu133plus (Affymetrix, Santa Clara, CA). The R Bioconductor package oligo (53) was used to create expression sets, perform the background correction and quantile-normalization per sample, as well as log-transform the data. The microarray data have been deposited in the public database Gene Expression Omnibus (GEO) (accession number: GSE222156). See Table 3 for gestational ages and corresponding cell numbers. We tested all genes on the array for differential expression between the fetal and the adult samples using a t-test for each gene separately and then applied the Benjamini-Hochberg procedure to adjust for multiple hypothesis testing. Probesets were annotated to Ensembl gene IDs and summaries are given on the level of Ensemble gene ids. Differentially expressed genes were defined as all genes with FDR < 5%.

Gene set enrichment analysis

Gene set enrichment analysis was performed using Webgestalt (54,55). All differentially expressed genes (FDR <5%) were used as input. All genes on the Hgu133plus array were used as background. The minimal gene set size was set to 2. Analyses were run separately for gene sets from the “biological process” and “molecular function” ontologies from Gene Ontology. The hypergeometric test was used to assess the significance of the overlap of the differentially expressed genes with each of the gene sets. The Benjamini-Hochberg procedure was applied to adjust for multiple hypothesis testing. Significant gene sets were defined as gene sets with FDR < 5%. None of the gene set of the “molecular function” ontology was significant.

Identification of RelB target genes

We obtained ChIP-seq peak calls of canonical and non-canonical subunits of NFKB (p65, p50, RelB and p52) measured in the lymphoblastoid cell line GM12878 (15). For each subunit we defined genes as bound if a binding site of the subunit localized within 1kb of the gene. Using Fisher’s exact test, we assessed whether binding sites for each subunit were overrepresented or depleted separately in the set of up and down regulated genes identified by the microarray analysis. Genes that were both differentially expressed and bound by a subunit were defined as target genes of the subunit.

Mice

C57Bl6 animals were purchased from Charles River and housed in the animal facility of the Biomedical Center in Munich at least one week before use in experiments. *Lyz2*^{GFP}, *Tnfaip3*$^{fl/fl}$ and *Ly6gCre* tdTomato (23,49,56,57) mice were generated as described before.

Generation of A20 overexpressing Hoxb8 cells and differentiation into neutrophil-like cells

The murine *pWPI-A20-IRES-EGFP* vector was a gift by A. Ma (University of California San Francisco, San Francisco, USA). The *pMSCV-Puro* and *pCL-Eco* vector were kindly provided by Hans Häcker (St. Jude Children's Research Hospital, Memphis, USA). For viral transduction, the coding region of *A20-IRES-EGFP* was cloned into the retroviral backbone *pMSCV-Puro*.

For virus production, human embryonic kidney (HEK) 293T cells (ATCC CRL-11268) were transfected with *pMSCV-A20-IRES-EGFP* and *pCL-Eco* using Lipofectamin 2000 (Thermo Fisher Scientific, Germany) according to the manufacturer's protocol. Virus-containing supernatant was harvested 48 h post transfection and Hoxb8-SCF cells, generated from C57Bl6 mice as described previously (58,59), were transduced by spinocculation using Lipofectamin®. Upon 72 h post transduction, puromycin-resistant cells were selected for the length of 7 d.

Differentiation of Hoxb8-SCF cells towards neutrophils was allowed by culture for 4 d in differentiation medium consisting of RPMI 1640 supplemented with 10% FCS, 1% Penicillin/Streptomycin, 20 ng/mL rmG-CSF (Peprotech) and 2% SCF-containing supernatant as described (60).

Purification of human and murine neutrophils

Human neutrophils were isolated from umbilical cord or peripheral venous blood by layering cells on a Polymorphprep density gradient (AXIS-SHIELD PoC AS, Dundee, Scotland) followed by centrifugation (500g, 30 min, room temperature). The neutrophil layer was harvested, washed with Dulbecco´s PBS and erythrocytes were lysed with ammonium chloride lysis buffer. Subsequently, neutrophils were purified by EasySep Human Neutrophil Enrichment Kit (Stem Cell Technologies). Alternatively, the EasySep™ Direct Human Neutrophil Isolation Kit (Stem Cell Technologies) was used. For quantitative Real-Time PCR analysis, purity was investigated by flow cytometry and required to be >90%.

Murine neutrophils were isolated from fetal blood by decapitation of C57Bl6 fetuses on embryonic day (E) 13.5/ E14.5 as well as E17.5/ E18.5. Blood was layered on a Percoll density gradient (Sigma-Aldrich, Germany). The neutrophil layer was isolated, washed with Dulbecco´s PBS and erythrocytes were lysed with ammonium chloride lysis buffer. To yield a highly pure cell population, neutrophils were further purified using the anti-mouse Ly6G-Pacific Blue antibody (BioLegend) by fluorescence activated cell sorting, using a BD FACS AriaIII instrument.

RNA processing and quantitative Real-Time PCR

RNA of neutrophils (>90% purity) was extracted with the RNeasy Mini Kit (Qiagen). RNA concentration and RNA concentration was measured with a Nanodrop instrument (ThermoFisher Scientific). Reverse transcription was conducted with High-Capacity cDNA Reverse Transcription Kit (Applied Biosystems) and quantitative real-time PCR was done using TaqMan Gene Expression Assays according to the manufacturer´s protocol (Applied Biosystems). Expression levels were calculated relative to house-keeping genes. See Table 4 for further detail.

Western Blot

Isolated human and murine neutrophils were homogenized in protein lysis buffer (150mM NaCl, 1% Triton X-100 (Applichem), 0,5% Na deoxycholate (Sigma-Aldrich), 50mM Tris-HCl pH7,3 (Merck), 2mM EDTA (Merck) supplemented with protease (Roche) and phosphatase inhibitors (Sigma-Aldrich) and proteins were resolved by SDS–polyacrylamide (SDS–PAGE) gels and then electrophoretically transferred from the gels onto PVDF membranes, which were subsequently blocked in LI-COR blocking solution (Lincoln, USA) and incubated with antibodies. The following antibodies were used for detection: mouse/rabbit anti- A20 (Abcam Cat: ab13597 and SantaCruz Cat: sc-166692), rabbit anti-p52 (CellSignaling Cat: 4882S), rabbit anti-pIκB (Cat: 2859) and rabbit anti-IκB (Cat: 4814) (Cell Signaling), mouse anti-GAPDH (Calbiochem, Cat: MAB374). IRDye 680RD (Cat: 926-68070) and IRDye800CW-(Cat: 925-32210) coupled secondary antibodies were purchased from LI-COR. Western blots were scanned using the Odyssey® CLx Imaging System (LI-COR) and analyzed with Image Studio software.

Imaging Flow Cytometry (AMNIS)

Human cord blood and peripheral blood neutrophils were isolated using the EasySep™ Direct Human Neutrophil Isolation Kit (Stem Cell Technologies). Afterwards, cells were fixed and permeabilized with the Foxp3 Transcription Factor Staining Buffer Set (Affymetrix, eBioScience) according to manufacturer´s protocol. Intracellular NF-κB was stained with the following antibodies: mouse anti-p65 (F-6) (Santa Cruz Cat: sc-8008 AF 488), mouse anti-Relb (Santa Cruz Cat: sc-48366 AF488), both conjugated with Alexa Fluor-488. DAPI (Invitrogen) was used to stain the nucleus. Images were acquired using an Amnis ImageStream multispectral imaging flow cytometer. Image analysis was done using the IDEAS software, applying the nuclear localization wizard. Similarity score defines the overlap of nuclear DAPI signal and NF-kB signal.

Flow Cytometry

Surface expression of TLR4 (anti-mouse TLR4-PE, BioLegend, Cat: 145403), LTβR (anti-mouse Cat: 134403 or anti-human Cat: 322008 LTβR-PE, Biolegend), TNFRI (TNFR I-APC, BioLegend Cat: 369906) or TNFRII (anti-mouse Cat: 113406 or anti-human Cat: B293743 TNFRII-PE-Cy7, BioLegend) was assessed on neutrophils from human cord or peripheral blood or mouse peripheral blood using a Beckman Coulter Gallios or a Cytoflex S flow cytometer and analyzed with the FlowJo Analysis Software. Surface expression of CD11b (Mac-1) (anti-mouse or anti-human Cd11b-AF700 BioLegend Cat: 101222) and CD18 (integrin ß2 subunit) (anti-human CD18-FITC, BioLegend Cat: 302106) were assessed after 2h of incubation either with 20 ng/ml recombinant human TNF-α or HBSS as control using Cytoflex S flow cytometer and FlowJo Analysis Software for analysis. Gating of human neutrophils was performed using CD15 (anti-human CD15-APC, BioLegend Cat: 323008) and CD66b (anti-human CD66b-PB, BioLegend Cat: 305112).

Flow Chamber

Ibidi flow chambers (0.5 µm Slide VI0.1) were coated with E-selectin (rhCD62E-Fc chimera, 5µg ml-1; R&D Systems), ICAM-1 (rhICAM-1, 4µg ml-1; R&D Systems) and CXCL-8 (rhCXCL-8, 10µg ml-1, Peprotech) overnight at 4°C. The next day, chambers were blocked with 5% Casein. Prior to the start of experiments, isolated human adult neutrophils were incubated for 2h with either HBSS (control) or adult or fetal serum, washed twice and then diluted in HBSS to $1x10^6$cells/ml. Perfusion through the flow chamber was conducted with a high precision pump (Harvard Apparatus) at a shear stress level of 1dyne cm-2.

Experiments were conducted on a ZEISS, AXIOVERT 200 microscope, provided with a ZEISS LD Plan-neofluor objective (20x, 0.4NA: and a SPOT RT ST Camera). MetaMorph software was used to generate movies for later analysis using Fiji software.

Phagocytosis

Human peripheral blood neutrophils were isolated using the EasySep™ Direct Human Neutrophil Isolation Kit (Stem Cell Technologies). Cells were stimulated for 2h with either RPMI (control), fetal or adult serum, washed two times and afterwards incubated with Zymosan particles for another 2h and further on processed as described in the data sheet (Phagocytosis Assay Kit (Green Zymosan)). Samples were analyzed in the FL1 channel of a Cytoflex S flow cytometer and data analyzed by FlowJo Analysis Software.

LT-α ELISA

Serum was obtained from human cord and adult peripheral blood. The assay was performed according to the manufacturer's instructions (R&D Systems). Samples were run in duplicates and analyzed using a microplate reader (TECAN).

Surgical preparation of the yolk sac and intravital microscopy

Pregnant *Lyz2*^{GFP} mice (E14.5-E17.5) were anesthetized intraperitoneally with 5 mg/ml ketamine and 1 mg/ml xylazine in 10 ml/kg of normal saline. Two hours prior to intravital microscopy, the uterine horn was carefully exteriorized through an abdominal wall incision followed by the intrauterine injection of either 100 µl LPS (1µg/µl in 0.9% NaCl), 50 µl of TNF-α (10ng/µl in 0.9% NaCl) or NaCl (0.9%). During the intrauterine injection between two fetuses, care was taken not to damage the fetuses or their surrounding yolk sacs. The site of injection between two fetuses was marked by a small knot using silk braided suture. Thereafter, the uterine horn was returned and the abdominal wall incision was temporarily closed by a small metallic clamp. After two hours, intravital microscopy to analyze leukocyte recruitment was performed as previously described (8) .

Intravital microscopy of TNF-α–stimulated mouse cremaster muscle venules

Mice were treated by intrascrotal injection of 500ng TNF-α (R&D Systems) 2h prior to microscopy, anesthetized and prepared for intravital microscopy, as described (61). Movies from cremasteric postcapillary venules ranging from 20-40µm in diameter were recorded using BX51WI microscope with a water immersion objective ×40, 0.80 NA and a Olympus CCD camera (CF8/1, Kappa). Blood samples were taken after the experiments and WBC and neutrophil counts were determined using ProCyte Dx Hematology Analyzer (IDEXX, Westbrook, USA). Rolling velocity and leukocyte adhesion efficiency (number of adherent cells/mm^2 divided by the systemic neutrophil count) were calculated on the basis of the recorded movies using Fiji software (62). Afterwards cremaster muscles were fixed with 4% PFA (AppliChem GmbH, Darmstadt, Germany) and stained using Giemsa (Merck Millipore, Darmstadt, Germany). The number of perivascular cells/mm^2 was calculated at the core facility bioimaging of the Biomedical Center with a Leica DM2500 microscope equipped with a DMC2900 CMOS camera and a HCX PL APO 100x/1.40 Oil Ph3.

Statistical analyses

All data were analyzed and plotted using Graph Pad Prism Software (GraphPad Software Inc.). For pairwise comparison of experimental groups, a paired t-test was performed, for comparison of independent samples, the unpaired student´s t-test was used. Depending on the condition, we used one-way analysis of variance with either Dunnett's post-hoc test (comparison of experimental groups against control) or Tukey's post-hoc test (comparison of all experimental groups against each other) or a two-way analysis of variance with Tukey's post-hoc test (comparison of paired experimental groups against each other) for multiple comparison. P-values <0.05 were considered statistically significant.

Study approval

All experiments using human cord blood were approved by the ethics committee of Ludwig-Maximilians-Universität München, project 249-08. All animal experiments were approved by the Regierung von Oberbayern, Germany (AZ 55.2-1-54-2531-80-76/12, 55.2-1-54-2532-102-2017 and 02-18-26).

Authors contribution

I.R., L.M.W. and K.H. designed and conducted experiments, analyzed data and wrote the manuscript. A.F., J.A. M.R. S.B., and M.Sa. acquired and analyzed data. C.N. and T.K. provided human cord blood samples, M.G., A.M. and C.S. provided mice. M.S-S and B.W. provided critical reagents and their expertise. T.S., L.K-H and M.H. analyzed data. M.Sp. designed experiments and wrote the manuscript.

Acknowledgements

We thank Dorothee Gössel, Sabine D'Avis, Anke Lübeck, and Nadine Schmidt for excellent technical assistance. We also thank Prof. Dr. Ludger Klein-Hitpass for his assistance with the transcriptome analysis. Work was supported by the German Research Foundation (DFG) collaborative research grant SFB914, projects A02 (to B.W.), A10 (to C.S.) and B01 (to M.Sp.), the core facility flow cytometry as well as the core facility bioimaging at the Biomedical Center, LMU, Planegg-Martinsried, Germany, and the Cell Analysis Core Facility at the TranslaTUM, Center for Translational Cancer Research, Technical University Munich, Germany.

Online Supplemental material

Supplemental Figure 1 shows purity and homogeneity of isolated neutrophils from peripheral adult and premature cord blood samples, as well as additional information on RelB and p65 protein levels and distribution. Supplemental Figure 2 displays surface expression of relevant NF-κB receptors and western blot analysis of fetal human neutrophils stimulated with adult serum. Supplemental Figure 3 supports the reported baseline activation of the adhesion cascade in *Tnfaip3*$^{fl/fl}$ *Ly6gCre* mice. Supplemental Movie 1 and 2 show reduced interaction of leukocyte with the yolk sac endothelial wall of E13.5 fetuses after LPS stimulation compared to E17.5. Supplemental Movie 3 shows increase adhesion of leukocytes in TNF-α stimulated cremaster muscle venules of *Tnfaip3*$^{fl/fl}$ *Ly6gCre* mice compared to *Ly6gCre* mice. Supplemental Table 1 displays all identified regulated genes, grouped according to their function. Supplemental Table 2 shows the overrepresentation of RelB subunit in promoters of upregulated genes. Supplemental Table 3 shows RelB-up and downregulated genes in cord blood neutrophils compared to adult neutrophils.

598 **Conflict of interest statement**

599 All authors have declared that no conflict of interest exists.

600

601 **Data availability statements**

602 The authors declare that the data supporting the findings of this study are available within the paper and
603 its Supplemental information files.

References

1. Stoll BJ, Hansen N, Fanaroff AA, et al. Late-onset sepsis in very low birth weight neonates: The experience of the NICHD Neonatal Research Network. *Pediatrics*. 2002;110(2 I):285-291. doi:10.1542/peds.110.2.285
2. Liu L, Oza S, Hogan D, et al. Global, regional, and national causes of under-5 mortality in 2000–15: an updated systematic analysis with implications for the Sustainable Development Goals. *Lancet*. 2016;388(10063):3027-3035. doi:10.1016/S0140-6736(16)31593-8
3. Levy O. Innate immunity of the newborn: Basic mechanisms and clinical correlates. *Nat Rev Immunol*. 2007;7(5):379-390. doi:10.1038/nri2075
4. Henneke P, Kierdorf K, Hall LJ, Sperandio M, Hornef M. Perinatal development of innate immune topology. *Elife*. 2021;10:1-21. doi:10.7554/eLife.67793
5. Burg ND, Pillinger MH. The neutrophil: Function and regulation in innate and humoral immunity. *Clin Immunol*. 2001;99(1):7-17. doi:10.1006/clim.2001.5007
6. Németh T, Sperandio M, Mócsai A. Neutrophils as emerging therapeutic targets. *Nat Rev Drug Discov*. 2020;19(4):253-275. doi:10.1038/s41573-019-0054-z
7. Nussbaum C, Gloning A, Pruenster M, et al. Neutrophil and endothelial adhesive function during human fetal ontogeny. *J Leukoc Biol*. 2013;93(2):175-184. doi:10.1189/jlb.0912468
8. Sperandio M, Quackenbush EJ, Sushkova N, et al. Ontogenetic regulation of leukocyte recruitment in mouse yolk sac vessels. *Blood*. 2013;121(21):e118-e128. doi:10.1182/blood-2012-07-447144
9. Lee AH, Shannon CP, Amenyogbe N, et al. Dynamic molecular changes during the first week of human life follow a robust developmental trajectory. *Nat Commun*. 2019;10(1). doi:10.1038/s41467-019-08794-x
10. Olin A, Henckel E, Chen Y, et al. Stereotypic Immune System Development in Newborn Children. *Cell*. 2018;174(5):1277-1292.e14. doi:10.1016/j.cell.2018.06.045
11. Zhong W, Danielsson H, Tebani A, et al. Dramatic changes in blood protein levels during the first week of life in extremely preterm infants. *Pediatr Res*. 2020;(January 2020). doi:10.1038/s41390-020-0912-8
12. Zhang Q, Lenardo MJ, Baltimore D. 30 Years of NF-κB: A Blossoming of Relevance to Human Pathobiology. *Cell*. 2017;168(1-2):37-57. doi:10.1016/j.cell.2016.12.012
13. Millet P, McCall C, Yoza B. RelB: an outlier in leukocyte biology. *J Leukoc Biol*. 2013;94(5):941-951. doi:10.1189/jlb.0513305
14. Yilmaz ZB, Weih DS, Sivakumar V, Weih F. RelB is required for Peyer's patch development: Differential regulation of p52-RelB by lymphotoxin and TNF. *EMBO J*. 2003;22(1):121-130. doi:10.1093/emboj/cdg004
15. Zhao B, Barrera LA, Ersing I, et al. The NF-κB Genomic Landscape in Lymphoblastoid B Cells. *Cell Rep*. 2014;8(5):1595-1606. doi:10.1016/j.celrep.2014.07.037
16. Ma A, Malynn BA. A20: Linking a complex regulator of ubiquitylation to immunity and human disease. *Nat Rev Immunol*. 2012;12(11):774-785. doi:10.1038/nri3313
17. Catrysse L, Vereecke L, Beyaert R, van Loo G. A20 in inflammation and autoimmunity. *Trends Immunol*. 2014;35(1):22-31. doi:10.1016/j.it.2013.10.005
18. Shembade N, Harhaj EW. Regulation of NF-κB signaling by the A20 deubiquitinase. *Cell Mol Immunol*. 2012;9(2):123-130. doi:10.1038/cmi.2011.59
19. Lee EG, Boone DL, Chai S, et al. Failure to regulate TNF-induced NF-κB and cell death responses in A20-deficient mice. *Science (80-)*. 2000;289(5488):2350-2354. doi:10.1126/science.289.5488.2350
20. Matmati M, Jacques P, Maelfait J, et al. A20 (TNFAIP3) deficiency in myeloid cells triggers erosive polyarthritis resembling rheumatoid arthritis. *Nat Publ Gr*. 2011;43(9).

652 doi:10.1038/ng.874
653 21. Blum KS, Pabst R. Keystones in lymph node development. *J Anat*. 2006;209(5):585-595.
654 doi:10.1111/j.1469-7580.2006.00650.x
655 22. Phillipson M, Heit B, Colarusso P, Liu L, Ballantyne CM, Kubes P. Intraluminal crawling of
656 neutrophils to emigration sites: a molecularly distinct process from adhesion in the recruitment
657 cascade. *J Exp Med*. 2006;203(12):2569-2575. doi:10.1084/jem.20060925
658 23. Faust N, Varas F, Kelly LM, Heck S, Graf T. Insertion of enhanced green fluorescent protein into
659 the lysozyme gene creates mice with green fluorescent granulocytes and macrophages. *Blood*.
660 2000;96(2):719-726. http://www.ncbi.nlm.nih.gov/pubmed/10887140
661 24. Orosz A, Walzog B, Mócsai A. In Vivo Functions of Mouse Neutrophils Derived from HoxB8-
662 Transduced Conditionally Immortalized Myeloid Progenitors. *J Immunol*. 2021;206(2):432-445.
663 doi:10.4049/jimmunol.2000807
664 25. Sperandio M, Smith ML, Forlow SB, et al. P-selectin glycoprotein ligand-1 mediates l-selectin-
665 dependent leukocyte rolling in venules. *J Exp Med*. 2003;197(10):1355-1363.
666 doi:10.1084/jem.20021854
667 26. Kan B, Razzaghian HR, Lavoie PM. An Immunological Perspective on Neonatal Sepsis. *Trends Mol*
668 *Med*. 2016;22(4):290-302. doi:10.1016/j.molmed.2016.02.001
669 27. Van Den Berg JP, Westerbeek EAM, Berbers GAM, Van Gageldonk PGM, Van Der Klis FRM, Van
670 Elburg RM. Transplacental transport of IgG antibodies specific for pertussis, diphtheria, tetanus,
671 haemophilus influenzae type b, and neisseria meningitidis serogroup C is lower in preterm
672 compared with term infants. *Pediatr Infect Dis J*. 2010;29(9):801-805.
673 doi:10.1097/INF.0b013e3181dc4f77
674 28. Sharma AA, Jen R, Butler A, Lavoie PM. The developing human preterm neonatal immune
675 system: A case for more research in this area. *Clin Immunol*. 2012;145(1):61-68.
676 doi:10.1016/j.clim.2012.08.006
677 29. Mariscalco MM, Tcharmtchi MH, Smith CW. P-selectin support of neonatal neutrophil adherence
678 under flow: Contribution of L-selectin, LFA-1, and ligand(s) for P-selectin. *Blood*.
679 1998;91(12):4776-4785. doi:10.1182/blood.v91.12.4776.412k32_4776_4785
680 30. Yost CC, Cody MJ, Harris ES, et al. Impaired neutrophil extracellular trap (NET) formation: A novel
681 innate immune deficiency of human neonates. *Blood*. 2009;113(25):6419-6427.
682 doi:10.1182/blood-2008-07-171629
683 31. Marcos V, Nussbaum C, Vitkov L, et al. Delayed but functional neutrophil extracellular trap
684 formation in neonates. *Blood*. 2009;114(23):4908-4911. doi:10.1182/blood-2009-09-242388
685 32. Weih F, Carrasco D, Durham SK, et al. Multiorgan inflammation and hematopoietic abnormalities
686 in mice with a targeted disruption of RelB, a member of the NF-κB/Rel family. *Cell*.
687 1995;80(2):331-340. doi:10.1016/0092-8674(95)90416-6
688 33. Weih F, Durham SK, Barton DS, Sha WC, Baltimore D, Bravo R. p50-NF-κB complexes partially
689 compensate for the absence of RelB: Severely increased pathology in p50(-/-)relB(-/-)double-
690 knockout mice. *J Exp Med*. 1997;185(7):1359-1370. doi:10.1084/jem.185.7.1359
691 34. Förster-Waldl E, Sadeghi K, Tamandl D, et al. Monocyte toll-like receptor 4 expression and LPS-
692 induced cytokine production increase during gestational aging. *Pediatr Res*. 2005;58(1):121-124.
693 doi:10.1203/01.PDR.0000163397.53466.0F
694 35. Sadeghi K, Berger A, Langgartner M, et al. Immaturity of infection control in preterm and term
695 newborns is associated with impaired Toll-like receptor signaling. *J Infect Dis*. 2007;195(2):296-
696 302. doi:10.1086/509892
697 36. Al-Hertani W, Sen RY, Byers DM, Bortolussi R. Human newborn polymorphonuclear neutrophils
698 exhibit decreased levels of MyD88 and attenuated p38 phosphorylation in response to
699 lipopolysaccharide. *Clin Investig Med*. 2007;30(2):44-53. doi:10.25011/cim.v30i2.979

37. Sharma AA, Jen R, Kan B, et al. Impaired NLRP3 inflammasome activity during fetal development regulates IL-1β production in human monocytes. *Eur J Immunol*. 2015;45(1):238-249. doi:10.1002/eji.201444707
38. Dinarello CA. Immunological and inflammatory functions of the interleukin-1 family. *Annu Rev Immunol*. 2009;27:519-550. doi:10.1146/annurev.immunol.021908.132612
39. Krikos A, Laherty CD, Dixit VM. Transcriptional activation of the tumor necrosis factor α-inducible zinc finger protein, A20, is mediated by κB elements. *J Biol Chem*. 1992;267(25):17971-17976. doi:10.1016/S0021-9258(19)37138-8
40. Song HY, Rothe M, Goeddel D V. The tumor necrosis factor-inducible zinc finger protein A20 interacts with TRAF1/TRAF2 and inhibits NF-κB activation. *Proc Natl Acad Sci U S A*. 1996;93(13):6721-6725. doi:10.1073/pnas.93.13.6721
41. Heyninck K, Beyaert R. The cytokine-inducible zinc finger protein A20 inhibits IL-1-induced NF-κB activation at the level of TRAF6. *FEBS Lett*. 1999;442(2-3):147-150. doi:10.1016/S0014-5793(98)01645-7
42. Yamaguchi N, Oyama M, Kozuka-Hata H, Inoue JI. Involvement of A20 in the molecular switch that activates the non-canonical NF-kB pathway. *Sci Rep*. 2013;3. doi:10.1038/srep02568
43. Vereecke L, Beyaert R, van Loo G. The ubiquitin-editing enzyme A20 (TNFAIP3) is a central regulator of immunopathology. *Trends Immunol*. 2009;30(8):383-391. doi:10.1016/j.it.2009.05.007
44. Lodolce JP, Kolodziej LE, Rhee L, et al. African-Derived Genetic Polymorphisms in TNFAIP3 Mediate Risk for Autoimmunity. *J Immunol*. 2010;184(12):7001-7009. doi:10.4049/jimmunol.1000324
45. Elsby LM, Orozco G, Denton J, Worthington J, Ray DW, Donn RP. Functional evaluation of TNFAIP3 (A20) in rheumatoid arthritis. *Clin Exp Rheumatol*. 2010;28(5):708-714.
46. Adrianto I, Wen F, Templeton A, et al. Association of a functional variant downstream of TNFAIP3 with systemic lupus erythematosus. *Nat Genet*. 2011;43(3):253-258. doi:10.1038/ng.766
47. Walle L Vande, Van Opdenbosch N, Jacques P, et al. Negative regulation of the NLRP3 inflammasome by A20 protects against arthritis. *Nature*. 2014;512(1):69-73. doi:10.1038/nature13322
48. Das T, Chen Z, Hendriks RW, Kool M. A20/tumor necrosis factor α-induced protein 3 in immune cells controls development of autoinflammation and autoimmunity: Lessons from mouse models. *Front Immunol*. 2018;9(FEB). doi:10.3389/fimmu.2018.00104
49. Tavares RM, Turer EE, Liu CL, et al. The Ubiquitin Modifying Enayme A20 Restricts B cell Survival and Prevents Autoimmunity. *Immunity*. 2010;27(33):181-191. doi:10.1016/j.immuni.2010.07.017.The
50. Hammer GE, Turer EE, Taylor KE, et al. Dendritic cell expression of A20 preserves immune homeostasis and prevents colitis and spondyloarthritis Gianna. *Nat Immunol*. 2011;12(12):1184-1193. doi:10.1038/ni.2135.Dendritic
51. Duong BH, Onizawa M, Oses-Prieto JA, et al. A20 Restricts Ubiquitination of Pro-Interleukin-1β Protein Complexes and Suppresses NLRP3 Inflammasome Activity. *Immunity*. 2015;42(1):55-67. doi:10.1016/j.immuni.2014.12.031
52. Walle L Vande, Van Opdenbosch N, Jacques P, et al. Negative regulation of the NLRP3 inflammasome by A20 protects against arthritis. *Nature*. 2014;512(1):69-73. doi:10.1038/nature13322
53. Carvalho BS, Irizarry RA. A framework for oligonucleotide microarray preprocessing. *Bioinformatics*. 2010;26(19):2363-2367. doi:10.1093/bioinformatics/btq431
54. Zhang B, Kirov S, Snoddy J. WebGestalt: An integrated system for exploring gene sets in various biological contexts. *Nucleic Acids Res*. 2005;33(SUPPL. 2):741-748. doi:10.1093/nar/gki475

748 55. Wang J, Duncan D, Shi Z, Zhang B. WEB-based GEne SeT AnaLysis Toolkit (WebGestalt): update
749 2013. *Nucleic Acids Res*. 2013;41(Web Server issue):77-83. doi:10.1093/nar/gkt439
750 56. Hasenberg A, Hasenberg M, Männ L, et al. Catchup: a mouse model for imaging-based tracking
751 and modulation of neutrophil granulocytes. *Nat Methods*. 2015;12(5):445-452.
752 doi:10.1038/nmeth.3322
753 57. Stremmel C, Schuchert R, Wagner F, et al. Yolk sac macrophage progenitors traffic to the embryo
754 during defined stages of development. *Nat Commun*. 2018;9(1). doi:10.1038/s41467-017-02492-
755 2
756 58. Wang GG, Calvo KR, Pasillas MP, Sykes DB, Häcker H, Kamps MP. Quantitative production of
757 macrophages or neutrophils ex vivo using conditional Hoxb8. *Nat Methods*. 2006;3(4):287-293.
758 doi:10.1038/nmeth865
759 59. Redecke V, Wu R, Zhou J, et al. Hematopoietic progenitor cell lines with myeloid and lymphoid
760 potential. *Nat Methods*. 2013;10(8):795-803. doi:10.1038/nmeth.2510
761 60. Zehrer A, Pick R, Salvermoser M, et al. A Fundamental Role of Myh9 for Neutrophil Migration in
762 Innate Immunity. *J Immunol*. 2018;201(6):1748-1764. doi:10.4049/jimmunol.1701400
763 61. Pruenster M, Kurz ARM, Chung KJ, et al. Extracellular MRP8/14 is a regulator of β2 integrin-
764 dependent neutrophil slow rolling and adhesion. *Nat Commun*. 2015;6:1-11.
765 doi:10.1038/ncomms7915
766 62. Schindelin J, Arganda-Carreras I, Frise E, et al. Fiji: an open source platform for biological image
767 analysis. *Nat Methods*. 2012;9(7):676-682. doi:10.1038/nmeth.2019.Fiji
768
769

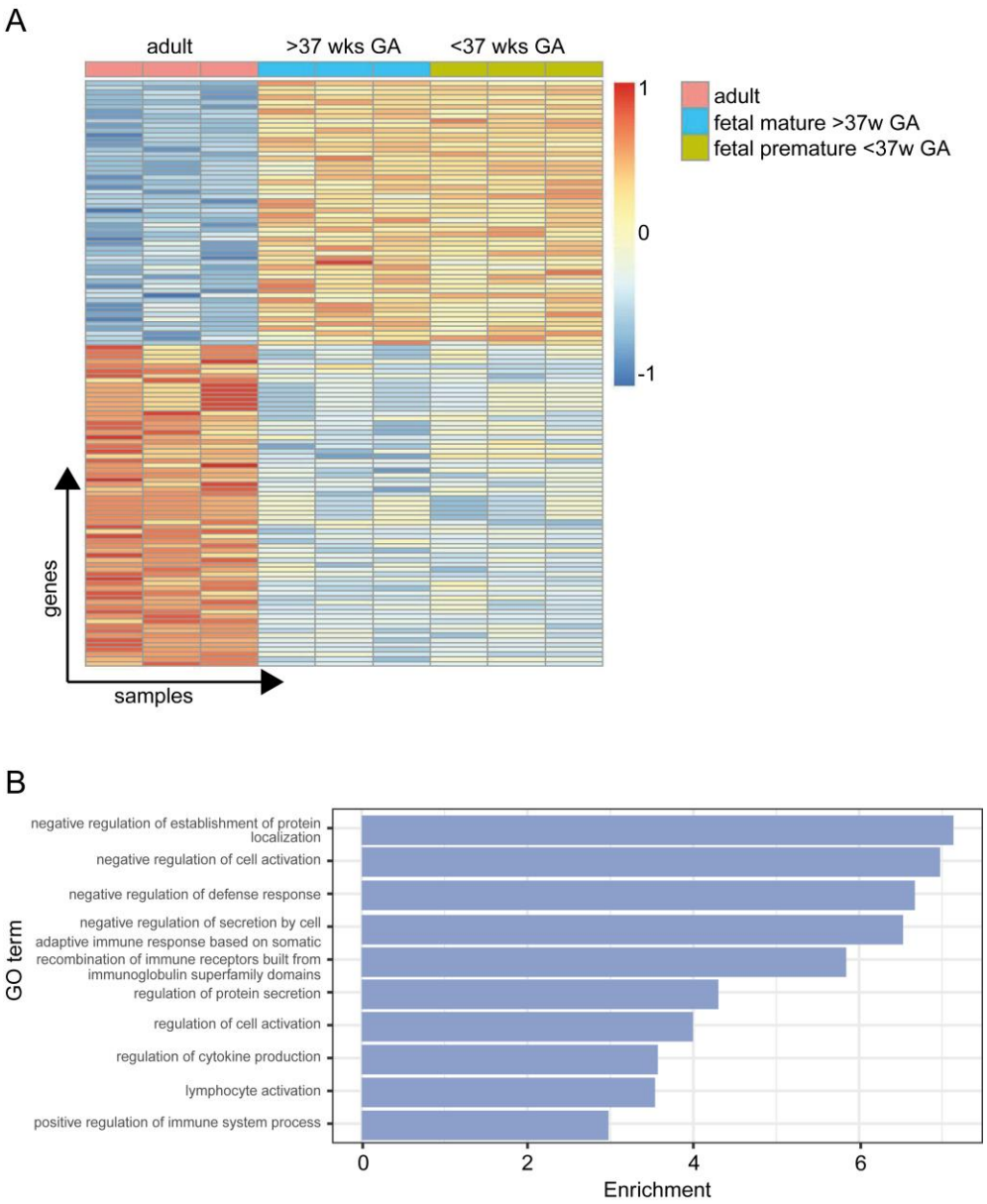

Figure 1: Differential gene expression signatures in human fetal and adult neutrophils.

(A) Neutrophils were isolated from peripheral blood of adult healthy donors and umbilical cord blood samples from mature fetuses (gestational age >37 weeks) or premature fetuses (gestational age <37 weeks) (n=3 per group). Differentially regulated genes between the samples are shown, each column representing one sample and each line one gene. Upregulated genes are depicted in red, whereas downregulated genes are depicted in blue. (B) Differentially expressed genes were used for gene set enrichment analysis. The bar plot shows the fold enrichment (x-axis) of the fraction of members of the gene set within all differentially expressed genes divided by the fraction of members of the gene set in the genome wide background set for each of the gene sets (y-axis), which are among the top 10 of all gene sets with FDR < 5%.

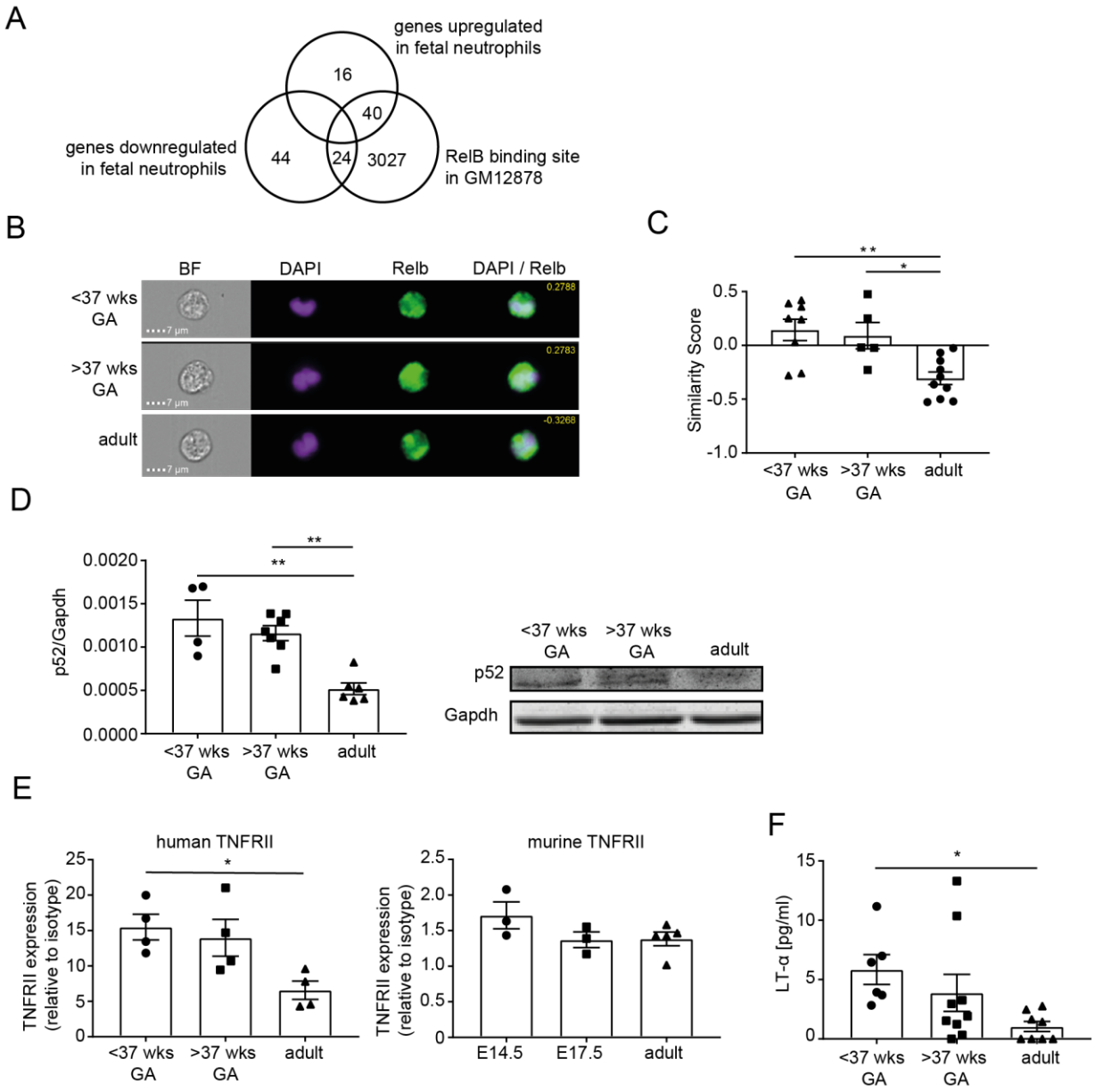

Figure 2: The non-canonical NF-κB subunit RelB determines a specific gene expression signature in fetal human neutrophils.

(A) Venn diagram representing the number of RelB regulated genes within all genes up- and downregulated in adult neutrophils in comparison to fetal neutrophils. Data was correlated with the published dataset of genome wide RelB binding sites in GM12878 human lymphoblastoid B cells (Zhao et al., 2014). (B) Imaging flow cytometry was performed on cord blood neutrophils from premature (gestational age <37 weeks) and mature (gestational age >37 weeks) fetal samples and peripheral blood from adult healthy donors. Nuclear signal was determined by DAPI and additionally the NF-κB subunit RelB was visualized. Representative pictures of fetal and adult neutrophils are shown as brightfield (BF) image, DAPI, NF-κB subunit RelB and a DAPI/RelB overlay. Respective similarity scores are displayed. Scale bar: 7µm. (C) Quantification of nuclear RelB. Similarity score defines overlap of nuclear DAPI signal and the respective NF-κB subunit. All data is presented as mean ± SEM. (* p<0.05, ** p<0.005, n= 5-10)

Ordinary one-way ANOVA with Tukey's multiple comparisons test. (D) Western blot and respective quantitative analysis of p52 in isolated neutrophils from premature (gestational age <37 weeks), mature (gestational age >37 weeks) and adult samples. Band intensity was normalized to Gapdh. All data is presented as mean ± SEM (** $p<0.005$, n= 4-7) Ordinary one-way ANOVA with Dunnett's multiple comparisons test. (E) Flow cytometry analysis of TNFRII expression on human and murine neutrophils out of whole blood from indicated gestational ages. Median fluorescence intensity normalized to isotype control is displayed. All data is presented as mean ± SEM (* $p<0.05$, n= 3-5) Ordinary one-way ANOVA with Dunnett's multiple comparisons test. (F) LT-α protein levels measured in cord blood serum from premature (gestational age <37 weeks) and mature infants (gestational age >37 weeks) and from whole blood of adult healthy donors by quantitative ELISA. Values are displayed in pg/ml. All data is presented as mean ± SEM. (** $p<0.005$, n= 6-9) Ordinary one-way ANOVA with Dunnett's multiple comparisons test.

806

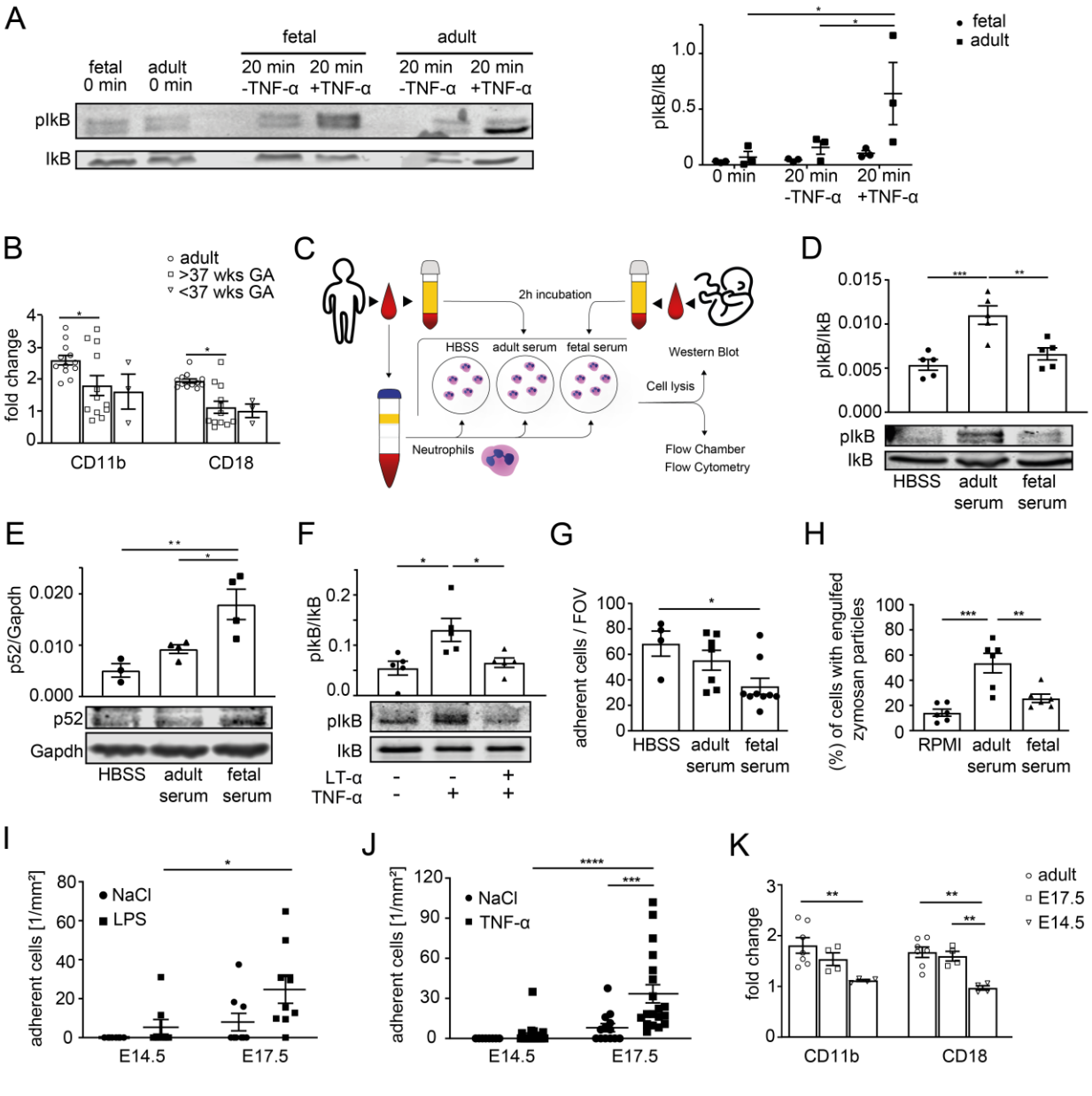
A
fetal
adult
fetal 0 min
adult 0 min
20 min -TNF-α
20 min +TNF-α
20 min -TNF-α
20 min +TNF-α
pIkB
IkB
pIkB/IkB
0 min
fetal
adult
B
adult
>37 wks GA
<37 wks GA
fold change
CD11b
CD18
C
2h incubation
HBSS
adult serum
fetal serum
Western Blot
Cell lysis
Neutrophils
Flow Chamber
Flow Cytometry
D
pIkB/IkB
HBSS
adult serum
fetal serum
E
p52/Gapdh
p52
Gapdh
F
pIkB/IkB
LT-α
TNF-α
G
adherent cells / FOV
H
(%) of cells with engulfed zymosan particles
RPMI
I
adherent cells [1/mm²]
NaCl
LPS
E14.5
E17.5
J
NaCl
TNF-α
K
fold change
E17.5
E14.5

807

Figure 3: Downregulation of the canonical NF-κB signaling pathway in fetal neutrophils.
(A) Western blot and respective quantitative analysis of IκB (Ser32) (40kDa) phosphorylation after TNF-α stimulation for indicated time periods in fetal (gestational age >37 weeks) and adult human neutrophils. Band intensities were normalized to total IκB protein. All data is presented as mean ± SEM. (* $p<0.05$, n= 3) Two-way ANOVA with Tukey's multiple comparisons test. (B) Quantitative analysis of Mac-1(CD11b/CD18) surface levels after 2h TNF-α stimulation in human adult, mature and premature fetal neutrophils by flow cytometry. Fold change indicates normalized values to Mac-1 surface levels after 2h HBSS incubation (control). All data is presented as mean ± SEM. (* $p<0.05$, n= 3-12). Two-way ANOVA with Tukey's multiple comparisons test. (C) Work flow of serum stimulation. Adult neutrophils were isolated from adult peripheral blood and stimulated for 2h with either HBSS or RPMI (control), fetal or adult serum and subsequently processed. (D) Western blot and respective quantitative analysis of phospho-IκB in adult neutrophils after HBSS (control) incubation or stimulation with adult or fetal serum. Band intensities were normalized to total IκB protein. All data is presented as mean ± SEM. (* $p<0.05$; n= 3-5) Ordinary one-way ANOVA with Tukey's multiple comparisons test. (E) Western blot and respective quantitative analysis of p52 in adult neutrophils after HBSS (control) incubation or stimulation with adult or fetal serum. Band intensities were normalized to Gapdh. All data is presented as mean ± SEM. (* $p<0.05$, ** $p<0.005$, n= 3-4). Ordinary one-way ANOVA with Tukey's multiple comparisons test (F) Western blot and respective quantitative analysis of IκB (Ser32) (40kDa) phosphorylation after incubation of human adult neutrophils with LT-α followed by TNF-α stimulation. Band intensities were normalized to total IκB protein. All data is presented as mean ± SEM. (* $p<0.05$; n= 5). Ordinary one-way ANOVA with Tukey's multiple comparisons test. (G) Adherent cells per field of view (FOV) in flow chambers coated with rhE-selectin, rhICAM-1 and rhIL8 after incubation of human adult neutrophils with either HBSS (control) or stimulation with adult or fetal serum. All data is presented as mean ± SEM. (* $p<0.05$; n= 4-9). Ordinary one-way ANOVA with Tukey's multiple comparisons test. (H) Quantitative analysis of phagocytosis of human adult neutrophils by measuring the amount of engulfed Zymosan particles by flow cytometry after incubation with either RPMI (control) or stimulation with adult or fetal serum. All data is presented as mean ± SEM. (** $p<0.005$, *** $p<0.001$; n= 6). Ordinary one-way ANOVA with Tukey's multiple comparisons test. (I) Adherent cells in yolk sac vessels in response to LPS were quantified and compared to adhesion induced by NaCl 0.9% injection. All data is presented as mean ± SEM. (* $p<0.05$, n=6-8 mice) Two-way ANOVA with Šídák's multiple comparisons test. (J) Adherent cells in yolk sac vessels in response to TNF-α were quantified and compared to adhesion induced by NaCl 0.9% injection. All data is presented as mean ± SEM. (*** $p<0.001$, **** $p<0.0001$, n=3-6 mice). Two-way ANOVA with Tukey's multiple comparisons test. (K) Quantitative analysis of Mac-1 (CD11b/CD18) surface levels after 2h TNF-α stimulation in murine adult and E14.5 and E17.5 fetal neutrophils by flow cytometry. Fold change indicates normalized values to Mac-1 surface levels after 2h HBSS incubation (control). All data is presented as mean ± SEM. (** $p<0.005$, *** $p<0.001$; n=3-12). Two-way ANOVA with Tukey's multiple comparisons test.

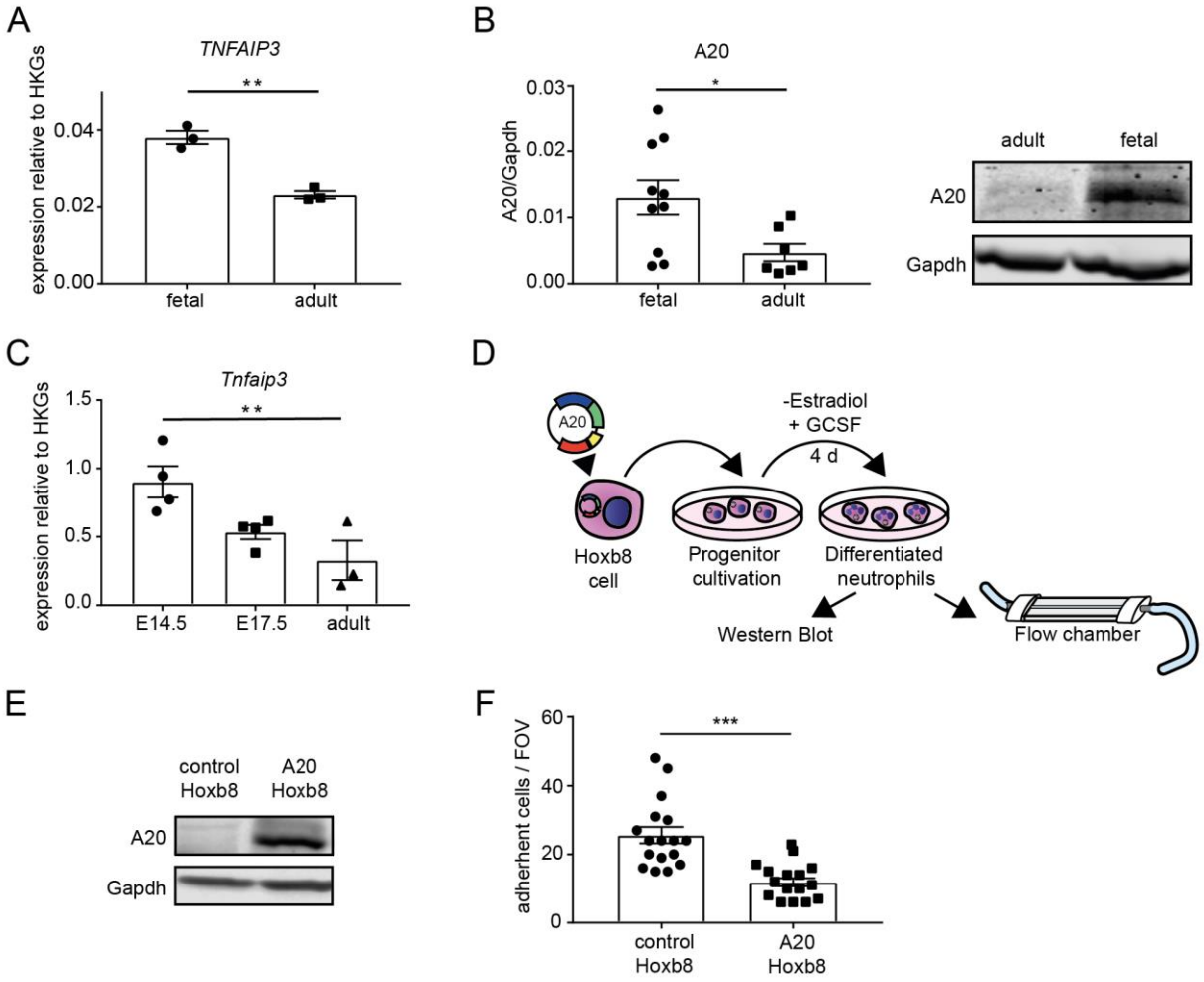

Figure 4: A20 upregulation in fetal neutrophils results in diminished adhesion.

(A) mRNA expression of *TNFAIP3* in fetal human neutrophils was compared to neutrophils isolated from peripheral blood of adult healthy donors by quantitative real time PCR. Expression is shown relative to the house keeping gene (HKG) *GAPDH*. (** p<0.005; n=3) Unpaired student´s t-test. (B) Western blot and respective quantitative analysis of A20 expression in neutrophils isolated from human fetal cord blood samples and neutrophils from adult peripheral blood. Band intensity was normalized to Gapdh protein. All data is presented as mean ± SEM. (* p<0.05, n= 8-10). Unpaired student´s t-test. (C) Expression of *Tnfaip3* mRNA relative to the house keeping genes (HKGs) *B2m* and *Gyk* in murine neutrophils was investigated by quantitative real time PCR in isolated neutrophils of E14.5 and E17.5 embryos and from the peripheral blood of adult mice. (** p<0.005; n=3-4). Ordinary one-way ANOVA with Dunnett's multiple comparisons test. (D)-Work flow of Hoxb8 experiments. Hoxb8 precursor cells overexpressing A20 and Hoxb8 control cells were differentiated into Hoxb8 neutrophils and subsequently flow chamber experiments were performed in addition to western blot verification of A20 overexpression. (E) Representative western blot image of A20 expression in control and A20 overexpressing Hoxb8 cells. Gapdh expression is displayed to ensure for equal loading. (F) Flow chamber analysis of differentiated Hoxb8 control and A20 overexpressing cell adhesion in microflow chambers coated with rmE-Selectin / rmICAM-1 and rmCXCL1. One representative field was recorded for 10min using an Olympus BX51WI

862 microscope with a CCD camera (model CF8/1, Kappa) and a water immersion objective (x40/0.8 NA,
863 Olympus). All data is presented as mean ± SEM. (*** $p<0.001$; n= 3). Unpaired Student´s t-test.
864

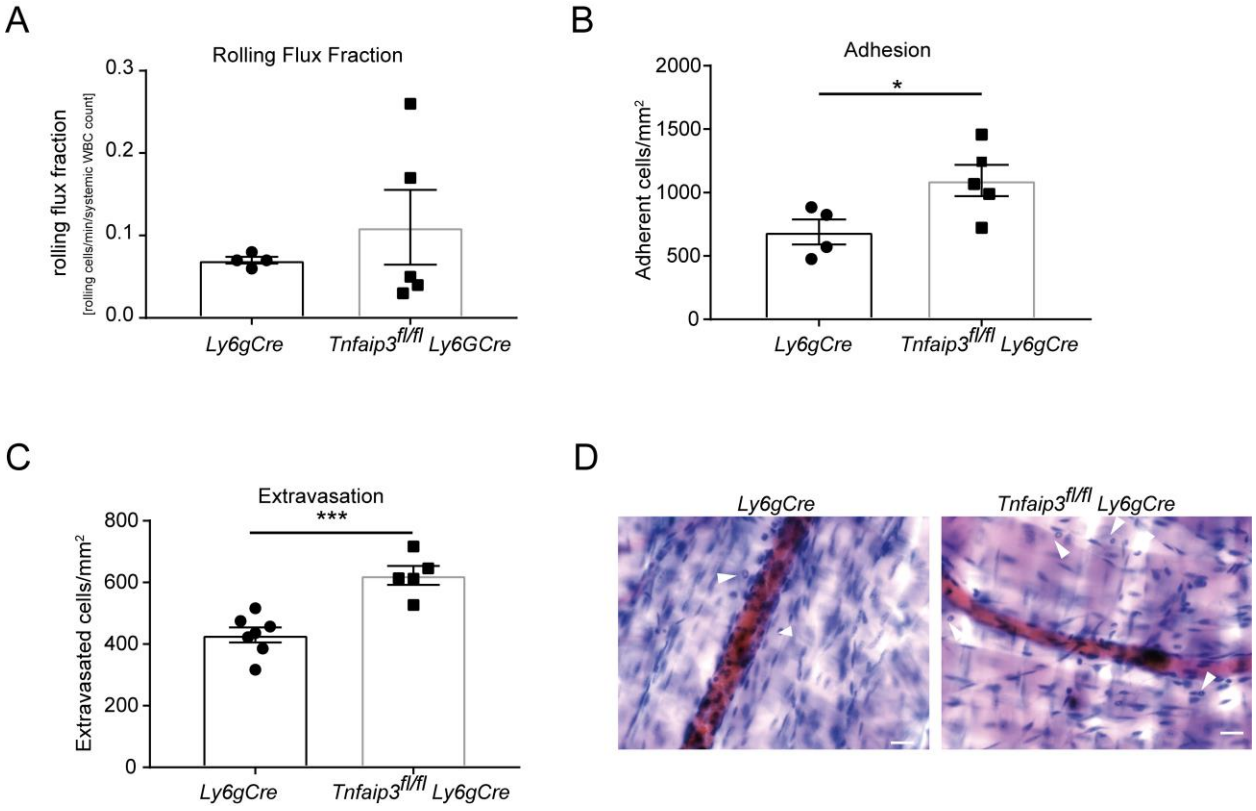

Figure 5: Increased neutrophil recruitment in *Tnfaip3*$^{fl/fl}$ *Ly6gCre* mice in vivo.

In vivo leukocyte rolling, adhesion and extravasation was analyzed in 2h TNF-α-stimulated venules of mouse cremaster muscles in *Ly6gCre* and *Tnfaip3*$^{fl/fl}$ *Ly6gCre* mice. (A) Rolling flux fraction (rolling cells/min divided by the total leukocyte flux), (B) adherent cells/mm^2, and (C) leukocyte extravasation in the perivascular region of Giemsa stained cremaster muscle whole mounts. 4 *Ly6GCre* (17 vessels) and 5 *Tnfaip3*$^{fl/fl}$ *Ly6gCre* (17 vessels) mice were analyzed. Values are given as mean ± SEM. (* $p<0.05$, *** $p<0.001$). Unpaired student´s t-test. (D) Representative images of Giemsa stained whole mounts of cremaster muscles of *Ly6gCre* and *Tnfaip3*$^{fl/fl}$ *Ly6gCre* mice. Arrows point to extravasated neutrophils. Scale bar: 30µm.

Table 1: Vessel parameters of *Ly6gCre* and *Tnfaip3*$^{fl/fl}$ *Ly6GCre* mice after TNF-α injection

	Diameter (µm)	Length (µm)	Centerline velocity (µm/s)	Shear rate (1/s)	Systemic WBC (K/µl)	Systemic neutrophil count (K/µl)
Ly6GCre	32.24 ± 1.41	260.95 ± 1.95	1826.09 ± 172.77	1441.65 ± 155.56	2.81 ± 0.2	0.64 ± 0.03
Tnfaip3*$^{fl/fl}$ *Ly6GCre	30.77 ± 0.98	258.51 ± 1.84	2142.14 ± 145.57	1717.18 ± 133.03	3.35 ± 0.4	0.79 ± 0.08

Table 2: Vessel parameters of *Ly6gCre* and *Tnfaip3*$^{fl/fl}$ *Ly6gCre* mice (Trauma)

	Diameter (µm)	Length (µm)	Centerline velocity (µm/s)	Shear rate (1/s)	Systemic WBC (K/µl)	Systemic neutrophil count (K/µl)
Ly6gCre	33.72 ± 1.47	260.01 ± 2.99	2554.55 ± 189.64	1924.61 ± 160.29	5.2 ± 0.4	1.6 ± 0.2
Tnfaip3*$^{fl/fl}$ *Ly6gCre	32.94 ± 0.92	259.12 ± 1.77	2005.13 ± 139.45	1511.13 ± 107.39	6.0 ± 0.7	1.0 ± 0.1

Table 3: Gestational ages and corresponding cell numbers used for microarray

Gestational age (weeks)	Cell number for microarray
32+4	$2x10^6$
32+0	$2x10^6$
30+5	$2x10^6$
40+2	$1x10^7$
38+0	$2x10^6$
38+6	$6x10^5$
Adult	$3x10^6$
Adult	$5x10^6$
Adult	$4x10^6$

Table 4: TaqMan expression assays used for quantitative real time PCR

TaqMan Expression Assay	Gene	Target species
Mm00518541_m1	IRAK-3	mouse
Mm00437121_m1	TNFAIP3	mouse
Mm00437762_m1	B2m	mouse
Mm00433896_m1	Gyk	mouse
Hs00936103_m1	IRAK-3	human
Hs00234713_m1	TNFAIP3	human
Hs02758991_g1	GAPDH	human
Hs01060665_g1	ACTB	human